41st Aerospace Sciences Meeting and Exhibit
6-9 January 2003, Reno, Nevada

AIAA 2003-625

PREDICTION OF STRUCTURAL BEHAVIOR OF JOINED-WING CONFIGURATION OF HIGH-ALTITUDE LONG-ENDURANCE (HALE) AIRCRAFT*

Soujanya Marisarla†, Vijay Narayanan††, Urmila Ghia‡, Karman Ghia§

Computational Fluid Dynamics Research Laboratory
Department of Mechanical, Industrial and Nuclear Engineering
§Department of Aerospace Engineering and Engineering Mechanics
University of Cincinnati
Cincinnati, OH 45221

ABSTRACT

The Air Force Research Laboratory (AFRL) has proposed a sensorcraft model with a joined-wing configuration for high-altitude long-endurance (HALE) aircraft. This aircraft operates at high altitudes and low speeds with high lift and minimum drag. These operating conditions require a lightweight aircraft with high-aspect-ratio wings. By virtue of their geometry, these wings are highly flexible, and exhibit significant structural deformations when subjected to aerodynamic loads during flight. Large deformations necessitate the consideration of nonlinear effects in the solution to compute the displacements more accurately. The aerodynamic loads are obtained from a CFD analysis that is being pursued in a concurrent effort at the University of Cincinnati. These aerodynamic loads are applied as input to the structural model, and a structural analysis of the wing is performed using ANSYS, a finite-element analysis software. The results for static linear and nonlinear as well as modal analyses are presented in this paper. The nonlinear analysis yields a lower value of deflection compared to the linear analysis. However, a change in the shape of the flow domain by this small magnitude could cause significant changes in the flow behavior. Hence, it is important to determine the displacements accurately, taking into account the nonlinearities arising in the model due to large deformations.

* This Research is supported, in part, by DAGSI Grant, VA-UC-00-03 and computational resources are provided by the Ohio Supercomputer Center.

† Research Assistant

†† Graduate Assistant

‡ Professor of Mechanical Engineering, Associate Fellow AIAA

§ Herman Schneider Professor of Aerospace Engg, Associate Fellow AIAA

INTRODUCTION

HALE aircraft, a subset of Unmanned Air Vehicles (UAV), have been developed primarily for surveillance and reconnaissance operations. To accomplish their mission requirements efficiently, HALE aircrafts are designed to loiter on station for long durations, and fly at high altitudes and low speeds to gain maximum ground coverage. These requirements necessitate a lightweight aircraft operating at high-lift and low-drag conditions, with high-aspect-ratio wings. By virtue of their high-aspect ratio geometry, such wings are highly flexible and experience significant deflections during normal flight operations when subjected to aerodynamic loads.

The major objective of this research is to determine the structural behavior of the Sensorcraft model [1,2], a current generation HALE aircraft shown in Fig. 1, and aid in design analysis of flexible aircraft vehicles.

The joined-wing design, shown in Fig. 2, is an innovative concept, which incorporates two wings that form a truss arrangement. Wolkovitch [3, 4] presents a detailed overview of the joined-wing concept with its advantages. The forward wing is swept back with a positive dihedral angle, and meets the aft wing, which is swept forward [5].

At the Computational Fluid Dynamics Research (CFDRL), University of Cincinnati, a CFD analysis is being currently pursued for steady and unsteady three-dimensional flow over the joined-wing model for various angles of attack (α) [6]. The structural response of the joined-wing model is examined using linear, nonlinear and modal analysis.

The joined wing is represented structurally by three different models – reinforced aerodynamic shell model, box-wing model, and solid-wing model. In the reinforced aerodynamic shell model, shown in Fig. 2, the surface grid used for CFD analysis is also used for the structural analysis. Even though in general, the fluid grid is finer than the structure, by retaining the same grid, the pressure distribution obtained from the

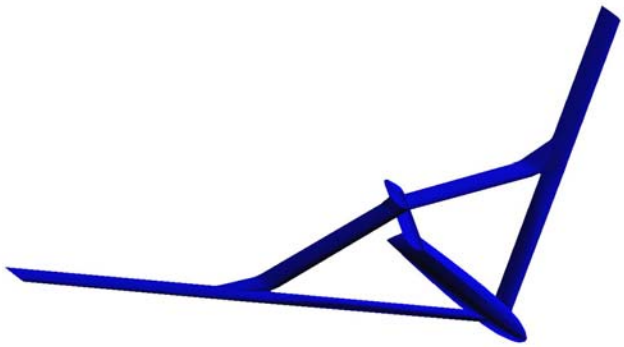

Fig. 1. Air Force Research Laboratory Sensorcraft Concept

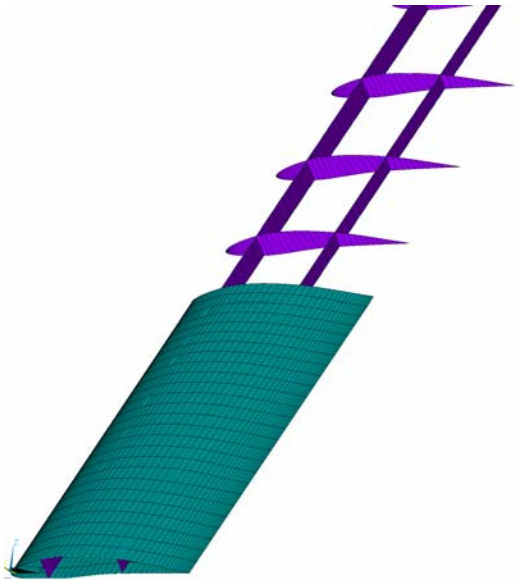

Fig. 2. Reinforced Shell Model with Ribs, Spars, Rods and Outer Skin

CFD analysis can be accurately transferred to the structure without the need for performing any interpolation. Reinforcements in the form of ribs, spars and rods are incorporated within this surface grid to provide the necessary stiffness to the structure. This model meets the requirements of having a lightweight structure, and represents a realistic wing by retaining the aerodynamic characteristics of the joined wing. Work is in progress to obtain the structural deformation of this model and hence, these results are not presented in this paper.

The box-wing concept is an equivalent representation of the joined-wing model. This Air Vehicles In-House Sensorcraft structure is modeled as a wing box with full structural details consisting of shear panels, rods, wing skins and structural masses. A modal analysis has been performed on this model and the results are included in this paper.

The solid wing model is used as first step to understand the structural behavior of the joined-wing model. The structure is modeled with solid elements without incorporating any reinforcements. The solid elements provide the necessary stiffness for the structure in the absence of the shear panel elements and rods. Detailed static linear and nonlinear as well as modal analysis results for this case are presented.

GOVERNING EQUATIONS

The governing equations of motion in finite-element form, derived from the principle of virtual work [7] are given as

$$[m]\{\ddot{d}\}+[c]\{\dot{d}\}+[k]\{d\}=\{f\} \qquad (1)$$

where $[m]$ - mass matrix,

$[c]$ - damping matrix,

$[k]$ - stiffness matrix,

$\{d\}$ - vector of nodal degrees of freedom,

$\{f\}$ - external load vector.

For a static problem, the displacement vector is independent of time, and the equilibrium equation is given by

$$[k]\{d\} = \{f\}. \qquad (2)$$

For a linear analysis, the stiffness matrix $[k]$ is independent of the displacement vector and Eq.(5) represents a system of simultaneous linear equations that can be solved to obtain the solution vector $\{d\}$.

However, for a nonlinear analysis, the stiffness matrix [k] is a function of the unknown displacement. Hence, the relationship between the displacement response d, and the applied load vector is nonlinear.

$$[k(d)]\{d\} = \{f\}. \qquad (3)$$

In designing structures, it is critical to know the natural frequencies of the structure. If a natural frequency of the structure is close to an excitation frequency, then severe vibration of the structure could occur, and to avoid these the natural frequencies of the structure must be altered by making suitable adjustments in the design. Modal analysis is used to determine the natural

frequencies of the structure. This is done by the use of Eq. (1) without any external loading or damping effects.

Hence, Eq. (1) reduces to

$$[m]\{\ddot{d}\}+[k]\{d\}=0\,. \qquad (4)$$

An undamped structure with no external loading experiences harmonic motion, and the solution to Eq. (2) is of the form

$$\{d\}=\{d_0\}\sin\omega t\,. \qquad (5)$$

Thus,

$$\left([k]-\omega^2[m]\right)\{d_0\}=\{0\}\,. \qquad (6)$$

Equation (4) represents an eigen problem and the eigenvalues, ω_i, that satisfy this equation are the natural frequencies of vibration of the system. The lowest nonzero eigenvalue is the fundamental vibration frequency. Corresponding to each eigenvalue, there exists an eigenvector $\{d_0\}_i$, a characteristic vibration mode.

STRUCTURAL MODEL

Figure 3 shows the CAD model of the joined wing. The wing span and chord are 535.4 in. and 50 in., respectively. The model is discretized into a number of 10-noded tetrahedral elements. Figure 4 shows the finite-element mesh comprised of 20664 grid points. Each of the 10 nodes in the tetrahedral has three translational degrees of freedom [8]. The material for the wing is generic aircraft-type aluminum. This material has excellent mechanical properties such as high strength and lightweight, and is ideal for the construction of airframes. The Young's Modulus of the material is 1E07 psi and the Poisson's ratio is 0.28. The aerodynamic loads determined from the CFD analysis performed at the University of Cincinnati are listed in Table 1. The lift forces are applied as pressures on the discretized model while the drag forces are applied as shear stress on the wing surface. The roots of the main and the aft wing are constrained in all degrees of freedom similar to that of a cantilever beam. The linear and the nonlinear system of equations given by Eqs. 5 and 6 are solved to obtain the unknown displacement vector. Solution of Eq. 6 has to be approached iteratively, and ANSYS uses the "Newton-Raphson" iterative scheme to solve nonlinear problems.

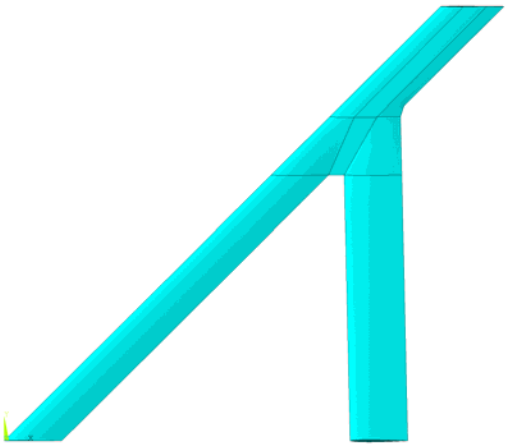

Fig. 3. CAD Model of Solid Joined Wing

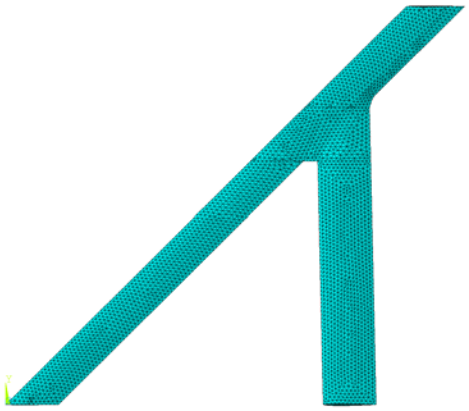

Fig. 4. Ten-Noded Tetrahedral Mesh for Solid Wing, 20664 nodes

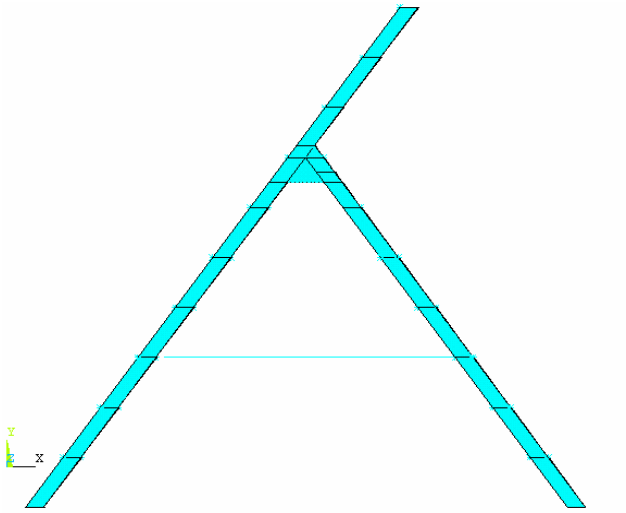

Fig. 5. Finite Element Mesh of Box-Wing Model

The aft wing in the joined wing plays a vital role in imparting stability to the model. To investigate this, a cantilever beam with dimensions and loading conditions similar to that of the main wing is analyzed. Since analytical results exist for a cantilever beam with

uniform loading, this problem also serves as a test case to ensure the correct usage of the software and validation of the code.

The box-wing model, shown in Figs. 5 and 6, consists of shear panels to represent the ribs and spars, which carry the shear loads, rods to represent the tension and compression, and wing skins on which the bending loads act. Masses are attached at specified locations in the box-wing model to account for the weight added by signal processing equipment, VHF antennae, fuel, etc. The fuselage and the tail of the two-fuselage Sensorcraft concept are modeled at about 30 feet away from the centerline of the aircraft. The symmetry of the aircraft permits modeling only one half of the total aircraft.

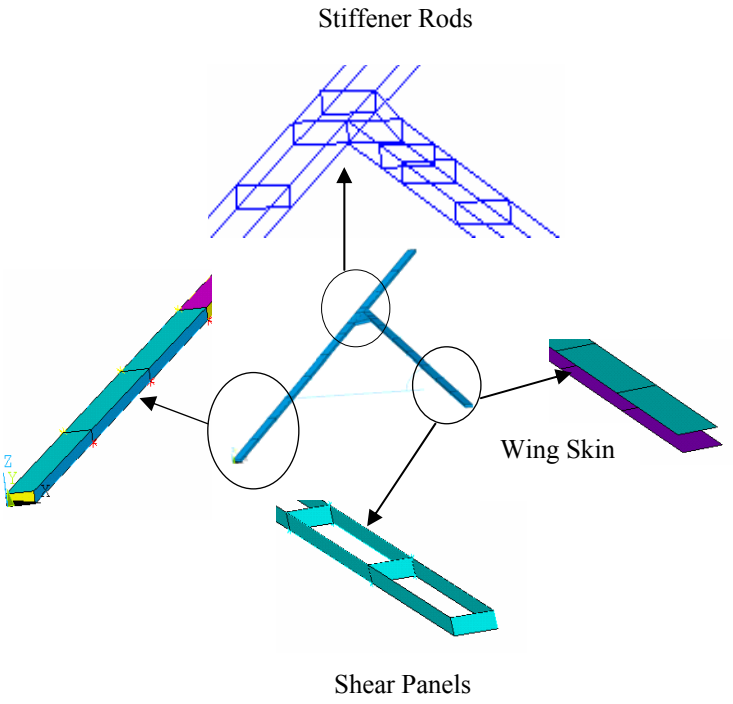

Fig. 6. Box-Wing with Rods, Shear Panels and Wing Skin

The box-wing model includes wing skins that are considerably thicker at the joint and at the roots or the centerline of symmetry where high stress concentrations are expected. Similarly, the spar rods at the roots of the wing and at the joint are thicker compared to those in other regions, in order to control localization of stress concentration at critical regions in the wing. A finite-element model of the box-wing is built in ANSYS using SHELL28 elements for shear panels, SHELL63 elements for the wing skin, LINK180 for the rods and MASS21 elements for the masses. Rigid elements are used to define and model the

Table 1. Aerodynamics of the Solid Joined-Wing model at $\alpha = -5°$

	PARAMETER	VALUE
1	Air density, ρ	4.33e-06 lb/cu.in
2	Velocity, V	4114.1732 in/s
3	Coefficient of Lift, C_L	0.5
4	Coefficient of drag, C_D	0.05
5	Lift force per unit area $\left(= 0.5 * \rho * V^2 * C_L\right)$	18.35 lbf/sq. in.
6	Drag force per unit area $\left(= 0.5 * \rho * V^2 * C_D\right)$	1.834 lbf/sq.in
7	Atmospheric pressure	0.797 psi

leading-edge and trailing-edge end points in order to interpolate and transfer the loads on the box-wing from aerodynamic analysis. A modal analysis is performed on the box-wing to determine the natural frequencies and mode shapes.

RESULTS

Test Case of Cantilever Beam

The tip deflection obtained from the finite-element analysis for the cantilever beam is 98.584 in. while the theoretical tip deflection is 100 in. The slight discrepancy of 1.4% between the theoretical and computed values of deflection shown in Table 2 is due to the fact that the cantilever plate has been modeled with solid tetrahedral elements instead of beam elements whose characteristics represent the beam theory more accurately than solid elements. The deflection obtained for a similar analysis when performed using beam elements was found to match the theoretical value with less than 0.01 % error [9]. Fig. 8a shows maximum deflection to be occurring at the free end of the beam. The stresses as shown in Fig. 8b are found to be maximum at the constrained end and minimum at the free end.

Table 2. Comparison of Theoretical and Finite-element values for a Cantilever Beam Tip Maximum Deflection

$\delta_{theoretical}$	$\delta_{computed}$	Deviation %
100 in.	98.584 in.	1.4

Solid-Element Joined Wing

For the joined wing solid model, the surface displacement for linear and nonlinear static analyses are shown by Figs. 9 and 11 while Figs. 10 and 12 show the surface stress distribution for linear and nonlinear static analyses. Again, similar to that of a cantilever beam, the deflections are found to be maximum at the free end. The stresses are maximum at the constrained end and in the region of the joint. The results for linear and nonlinear analyses are summarized in Table 3. The maximum tip deflection obtained from linear analysis is 70.489 in. whereas the nonlinear analysis yields a maximum value of 68.418 in. A nonlinear analysis of this geometry yields a smaller value of displacement than a linear analysis. This is because, in large displacement analysis, as the wing deflects, a portion of the load places the beam in tension and tends to stiffen the beam in bending.

Table 3. Comparison between Results of Linear and Nonlinear Structural analyses for Solid Joined-Wing Model

	Linear Analysis	Nonlinear Analysis
Maximum von Mises Stress (psi)	322111	322194
Maximum Deflection (in.)	70.489	68.418

The joint in the wing plays a vital role in reducing the deflection at the tip. The test case geometry has the same dimensions as that of the main wing and was subjected to similar loads. The deflection was close to 100 in., but the deflection at the tip for the joined wing is only around 70 inches. The presence of the joint clearly decreases the deflection at the tip but at the cost of increased stress levels. The importance of the auxiliary wing is further established by Fig. 13, which shows the displacement versus distance along the span of the leading edge for the linear and nonlinear analyses. The deflection is initially zero at the constrained end, and increases with distance along the span and reaches the maximum level at the free tip. However, there is noticeable retardation in the slope of the curve about half way along the span, indicating the role of joint in reducing the large deflections expected in long and slender structures.

Table 4. Natural Frequencies of the Solid Joined-Wing Model

Mode Number	Natural Frequency (Hertz)
1	0.10515
2	0.25483
3	0.39630
4	0.64369
5	0.96010
6	1.11250

Table 4 shows the natural frequencies of the structure obtained from the modal analysis. From the mode shapes shown in Fig. 14, it is clear that the effect of the second structure at the joint reduces the vertical displacement of the wing. The deflection is less at the constrained roots of the wing and tends to increase towards the free end of the wing, which is the characteristic of a fixed-free structure. It is also seen that the effect of the joint is more greatly pronounced for higher mode shapes. At higher modes, the rear portion of the wing reduces the vertical displacement of the forward wing portion and also induces a twisting motion. This twist causes stress concentration in the joint.

Box-Wing Model

The preliminary results obtained from the modal analysis of box-wing model [10] are presented in this work. Symmetry boundary conditions are imposed for this modal analysis. The Block Lanczos method is applied and first five modes are extracted. The first two modes obtained are rigid body modes. Table 5 shows the natural frequencies of the box-model obtained from the modal analysis. As in the case of the solid model from the mode shapes shown in Figs. 15, it is seen that the effect of the joint is more greatly pronounced for higher mode shapes where the rear portion of the wing reduces the vertical displacement of the forward wing portion and also induces a twisting motion.

The results are compared with the NASTRAN model results [11]. Though within the same range, the disparity in the values of the frequencies obtained is attributed to the issues faced in importing and translating the NASTRAN RBE1 elements into ANSYS, which are currently under investigation.

Table 5. Natural Frequencies of the Box-Wing

Mode Number	Natural Frequency (Hertz)	
	NASTRAN	ANSYS
1	0	0
2	0	0
3	1.3134	0.9909
4	1.5751	1.3826
5	2.2101	1.8130

CONCLUSION

Linear and nonlinear static analyses are performed on the joined-wing configuration using ANSYS. Results are obtained for deflections and stress distributions. Large deflections are typical in long, slender wings and can be effectively reduced by joined-wing design, though at the cost of increased stress levels at the joint. The difference between the values of maximum deflection obtained from linear and nonlinear analysis is only about 2%. However, a change in the shape of the flow domain by this small magnitude could cause significant changes in the flow behavior. Hence it is important to determine the displacements accurately, taking into account the nonlinearities arising in the model due to large deformations.

In the reinforced shell model, shown in Fig. 2, the aspect ratio of some elements along the leading and trailing edge violate shape warnings. Work is in progress to improve the quality of these elements to get accurate results for the structural analysis.

A complete, aeroelastic analysis of the Sensorcraft configuration will be performed by interfacing the structural and CFD solvers along with a grid generator within MDICE frame work.

REFERENCES

1. Johnson, F. P., "Sensorcraft: Tomorrow's Eyes and Ears of the Warfighter," AIAA-2001-4370, August, 2001.
2. Blair M., Moorhouse D., Weisshaar T., (2000), "System Design Innovation using Multi-Disciplinary Optimization and Simulation," AIAA-2000-4705.
3. Wolkovitch, J., (1986) "The Joined Wing: An Overview," *Journal of Aircraft*, Vol. 23, pp. 161-178.
4. Wolkovitch, J., (1987) "A second look at the Joined Wing," *Proceedings of NUUL SymposiumDelft University Press*.
5. Tyler, C., Schwabacher, G., Carter, D., (2002), "Comparison of Computational and Experimental Studies for a Joined-Wing Aircraft," *40th AIAA Aerospace Science Meeting & Exhibit,* January, Reno, NV, AIAA 2002-0702.
6. Sivaji, R., Ghia, U., Ghia, K., Thornburg, H., (2003), "Aerodynamic Analysis of the Joined-Wing Configuration of a HALE Aircraft," *41st AIAA Aerospace Science Meeting & Exhibit,* January, Reno, NV, AIAA 2003-0606.
7. Cook, R. D., Malkus, D. S., Plesha, M. E., (1989), Concepts and applications of finite element analysis, Wiley, 3rd ed.
8. ANSYS 6.1 Reference Manual, ANSYS Inc. 2001
9. Marisarla, S., Narayanan, V., Ghia, U. and Ghia, K., (2002), "Structural Analysis of Joined Wing of High-Altitude Long-Endurance (HALE) Based on the Sensor-Craft Configuration," AIAA Mini-symposium, Dayton, OH, Book of Abstracts.
10. Reich, G., (2002), "VA In-house Sensorcraft Box-Wing Configuration," Private Communication.
11. Huttsell, L., "NASTRAN Box-Wing Vibrational Analysis Results," Private Communication.

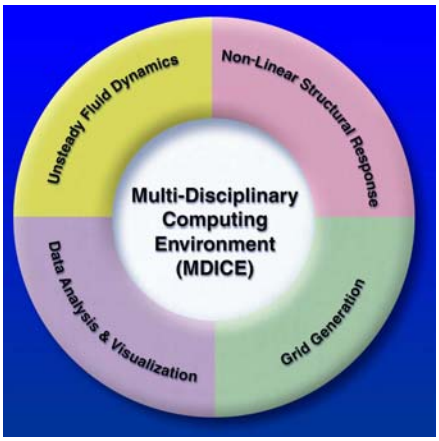

Fig. 7. MDICE Frame Work

ACKNOWLEDGEMENTS

The authors are grateful for DAGSI sponsorship under task VA-UC-00-03, monitored by Dr. Larry Huttsell of the AFRL. This work is also supported in part by a grant of computer resources provided by the Ohio Super Computer center. Authors would like to thank Dr. Phil Beran and Dr. Gregory Reich of the AFRL for their assistance to various aspects of the project.

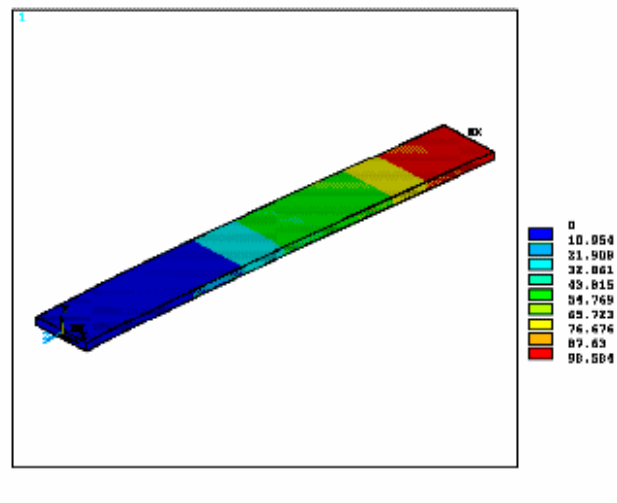

Fig. 8a. Deflection for Cantilever Beam

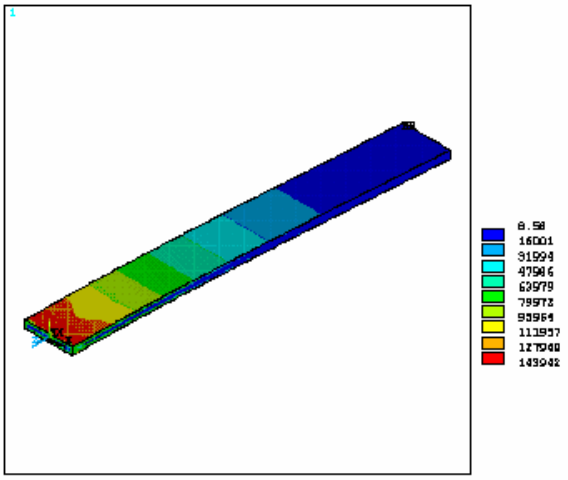

Fig. 8b. Stress Distribution for Cantilever Beam

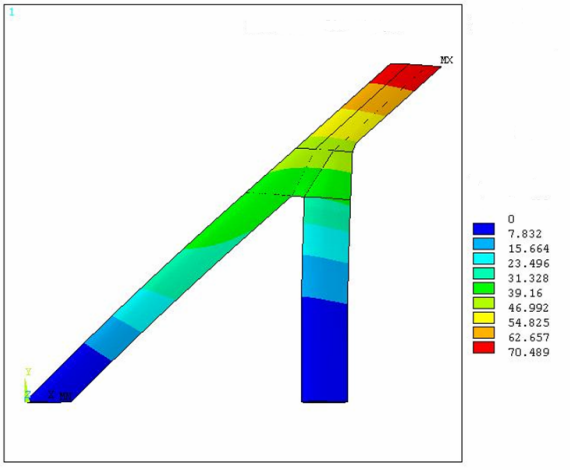

Fig. 9. Deflection from Linear Analysis for Solid Wing

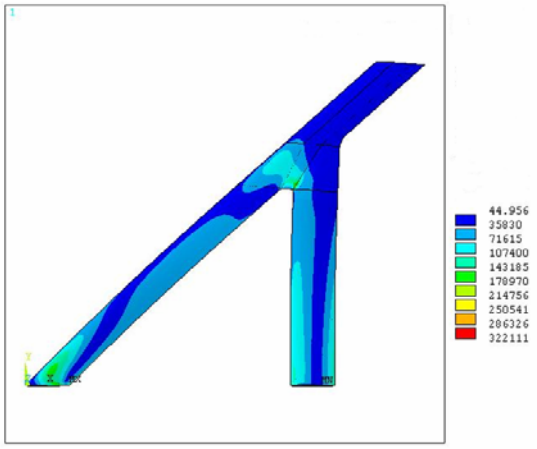

Fig. 10. von Mises Stress from Linear analysis for Solid Wing

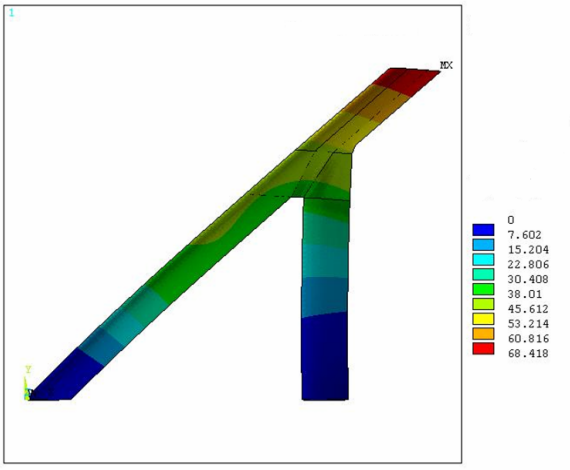

Fig. 11. Deflection from Nonlinear Analysis for Solid Wing

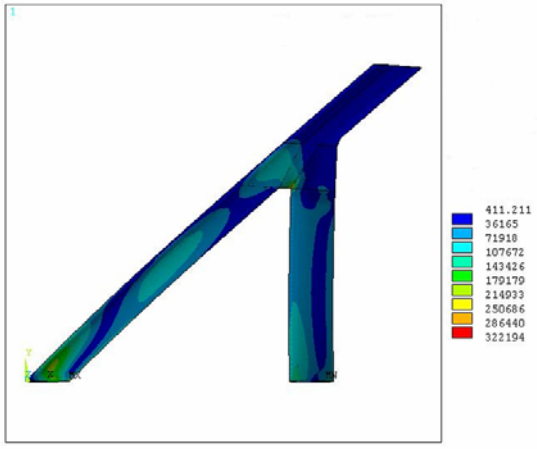

Fig. 12. von Mises Stress from Nonlinear analysis for Solid Wing

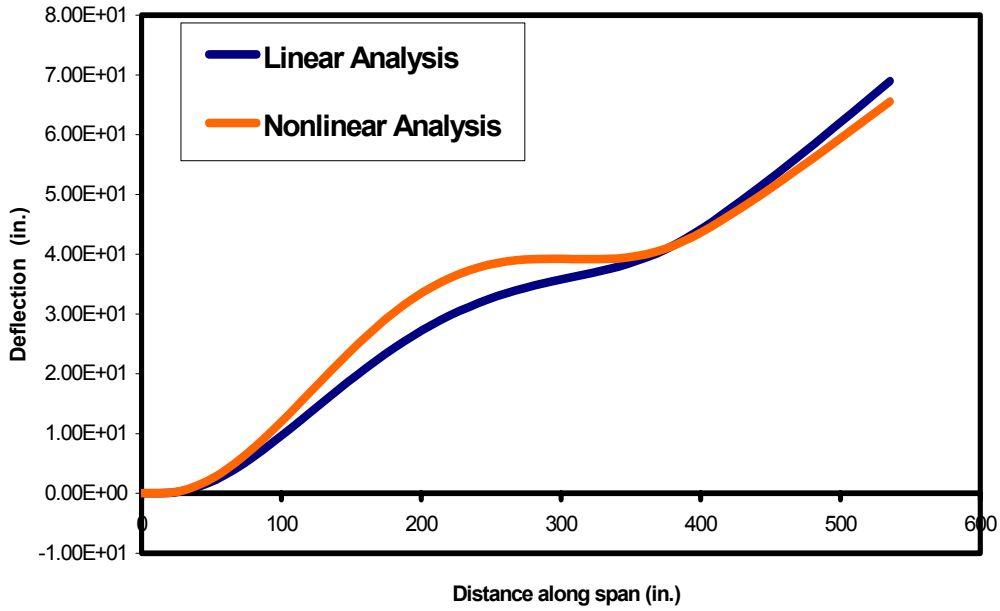

Fig. 13. Deflection versus Distance along Span for Linear and Nonlinear Analyses

Mode shape 1
0.10515 Hz

Mode shape 2
0.25483 Hz

Mode shape 3
0.39630 Hz

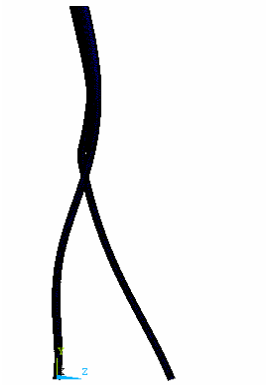

Mode Shape 4
0.64369 Hz

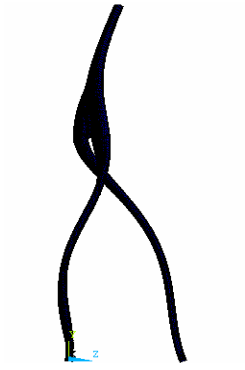

Mode Shape 5
0.96010 Hz

Mode shape 6
1.11250 Hz

Fig. 14. Mode Shapes for the Solid Wing with Clamped Boundary Condition (1-6)

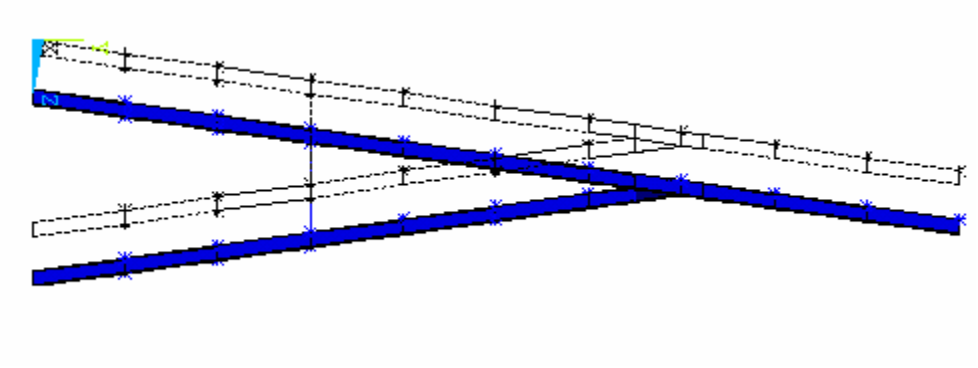

Mode Shape 1
0 Hz

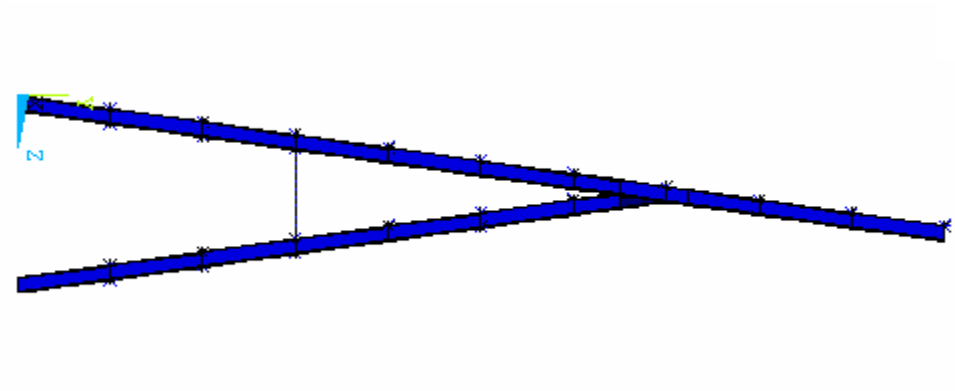

Mode Shape 2
0 Hz

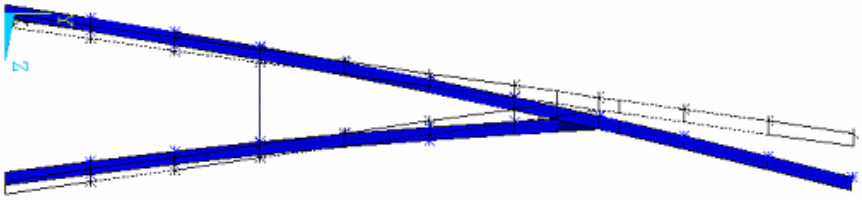

Mode Shape 3
0.9909 Hz

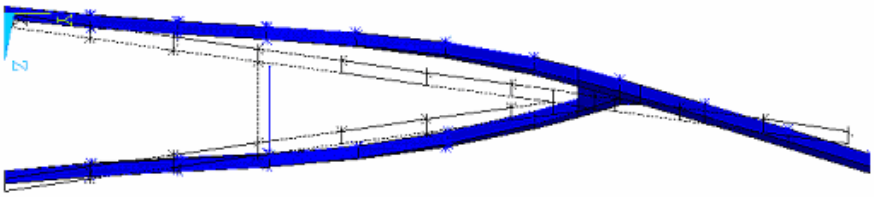

Mode Shape 4
1.3826 Hz

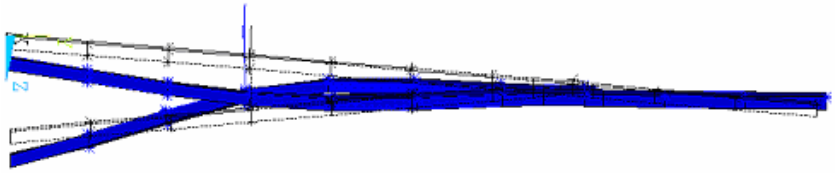

Mode Shape 5
1.813 Hz

Fig. 15. Three flexible modes of Box-Wing model. Symmetric conditions result in mode Shapes 1 & 2 as rigid body modes with translations.